

# Inhomogeneous accretion discs and the soft states of black hole X-ray binaries

Jason Dexter<sup>1\*</sup> and Eliot Quataert<sup>1</sup>

<sup>1</sup>*Department of Astronomy and Theoretical Astrophysics Center, University of California, Berkeley, CA 94720-3411, USA*

27 September 2018

## ABSTRACT

Observations of black hole binaries (BHBs) have established a rich phenomenology of X-ray states. The soft states range from the low variability, accretion disc dominated thermal (TD) state to the higher variability, non-thermal steep power law state (SPL). The disc component in all states is typically modeled with standard thin disc accretion theory. However, this theory is inconsistent with optical/UV spectral, variability, and gravitational microlensing observations of active galactic nuclei (AGNs), the supermassive analogs of BHBs. An inhomogeneous disc (ID) model with large ( $\simeq 0.4$  dex) temperature fluctuations in each radial annulus can qualitatively explain all of these AGN observations. The inhomogeneity may be a consequence of instabilities in radiation-dominated discs, and therefore may be present in BHBs as well. We show that ID models can explain many features of the TD and SPL states of BHBs. The observed relationships between spectral hardness, disc fraction, and rms variability amplitude in BHBs are reproduced with temperature fluctuations similar to those inferred in AGNs, suggesting a unified picture of luminous accretion discs across orders of magnitude in black hole mass. This picture can be tested with spectral fitting of ID models, X-ray polarization observations, and MHD simulations of radiation-dominated discs. If BHB accretion discs are indeed inhomogeneous, only the most disc-dominated states (disc fraction  $\gtrsim 0.95$ ) can be used to robustly infer black hole spin using current continuum fitting methods.

**Key words:** accretion, accretion discs — black hole physics — X-rays: binaries

## 1 INTRODUCTION

Spectral and timing observations of black hole X-ray binaries (BHBs) in the energy range  $\sim 1 - 100$  keV have established characteristic outburst “states” common to many sources (e.g., Remillard & McClintock 2006, hereafter RM06). The “thermal” (TD) state has little variability, and a large fraction of the integrated flux is well described by a standard thin black hole accretion disc model (NT, Shakura & Sunyaev 1973; Novikov & Thorne 1973). The “low/hard” state is characterized by a hard power law spectrum with a weak, soft disc component. It is often modeled as a thin disc truncated well outside of the black hole marginally stable orbit. Inside of this location, the accretion flow is assumed to be geometrically thick and radiatively inefficient (Esin, McClintock & Narayan 1997). The “steep power law” state (SPL) is characterized by a soft (photon index  $\Gamma > 2.4$ ) power law extending unbroken to  $\lesssim 1$  MeV (Grove et al. 1998). Its physical origin remains uncertain.

This common interpretation of the X-ray states relies on the validity of the NT model. However, this model is theoretically inconsistent in the TD and SPL states when the disc extends down to the marginally stable orbit of the black hole. In these luminous in-

ner regions, radiation pressure provides the vertical support against gravity, and the NT model is both thermally (Shakura & Sunyaev 1976) and viscously (Lightman & Eardley 1974) unstable. Global MHD simulations of thin discs (Penna et al. 2010; Sorathia et al. 2012, and references therein), which include the physics of angular momentum transport via the magnetorotational instability (Balbus & Hawley 1991), do not include radiation pressure and therefore cannot test the validity of the NT model. Local MHD simulations find that small patches of radiation-dominated discs are thermally stable (Hirose, Krolik & Blaes 2009), but suggest that the viscous (Lightman-Eardley) instability may operate (Hirose, Blaes & Krolik 2009). This instability has also been proposed as a model for spectral state transitions in GRS 1915+105 (Belloni et al. 1997; Neilsen, Remillard & Lee 2012).

The NT model is disfavored by optical/UV observations of active galactic nuclei (AGNs) with similar  $L/L_{\text{edd}}$  to the soft, luminous states of BHBs. The model underproduces the observed UV emission (Zheng et al. 1997) and requires a relativistic mechanism to explain the simultaneous variability observed at well separated optical wavelengths (Krolik et al. 1991). Recent microlensing observations find that quasar accretion discs are a factor of  $\sim 4$  larger than predicted by the NT model (Jiménez-Vicente et al. 2012, and references therein). Dexter & Agol (2011, hereafter DA11) showed

\* E-mail: jdexter@berkeley.edu

that a disc with large, local temperature fluctuations ( $\simeq 0.4$  dex) can explain all of these observations. The fluctuations could be driven by instabilities in radiation pressure dominated discs, in which case they would operate in BHBs as well.

In this Letter, we propose a novel interpretation of the soft, luminous TD to SPL states of BHBs in terms of this inhomogeneous accretion disc model (ID, summarized in §2). We show how interpreting ID spectra with the standard NT model can explain the X-ray spectral and variability properties of soft BHBs (§3). In §4 we assess the requirements for the ID model to fit observed BHB X-ray spectra. Inhomogeneity also may have important implications (§5) for the continuum fitting method for measuring black hole spin (CF, McClintock et al. 2011, and references therein). We discuss the prospects for testing BHB accretion disc inhomogeneity observationally and theoretically in §6.

## 2 INHOMOGENEOUS ACCRETION DISCS

DA11 proposed a toy model of an inhomogeneous accretion disc. The disc is taken to be optically thick everywhere so that its flux is specified completely by the effective temperature,  $T(r, \phi, t)$ . The radial temperature profile is set by assuming that the model reproduces the NT surface brightness when averaged over azimuth and time. Retaining the NT model on average is motivated theoretically by conservation laws and numerical simulations (Hirose, Blaes & Krolik 2009), and is consistent with quasar microlensing observations (Eigenbrod et al. 2008). DA11 broke the disc into independently fluctuating zones spaced evenly in  $\log r$  and  $\phi$ , with  $n$  total zones per octave in radius. Motivated by results from quasar variability (e.g. Kelly, Bechtold & Siemiginowska 2009; MacLeod et al. 2010), each zone performs a “damped random walk” in  $\log T$  around the local thin disc value with amplitude  $\sigma_T$  in dex and timescale  $t_{\text{drw}}$ . Both of these quantities are assumed constant in radius, and the results are insensitive to  $t_{\text{drw}}$ . The resulting power spectra are broadly consistent with those observed in BHBs (Kelly, Sobolewska & Siemiginowska 2011), but do not include the high frequency quasi-periodic oscillations often seen in the SPL.

For a fixed number of zones, the rms variability increases with increasing  $\sigma_T$ . We fix  $n = 1000$  (see §3), in which case the rms is well fit by the empirical formula (cf. equation 1 of DA11),

$$\text{rms} \simeq 0.02 \sqrt{\exp(16\sigma_T^2) - 1} \quad (1)$$

In the limit  $n \rightarrow \infty$ , this time-dependent model leads to a stationary flux profile depending only on  $r$  and  $x \equiv \ln(10) \sigma_T$ :

$$F_\nu(r; \sigma_T) = \frac{2\pi h\nu^3}{f^4 c^2} \int_0^\infty \frac{dw}{\sqrt{\pi} x w} \frac{e^{-[\ln w + x^2]^2/x^2}}{e^{z/w} - 1}, \quad (2)$$

where  $F_\nu$  is the flux at frequency  $\nu$  and  $z \equiv h\nu/kfT$ . The effective temperature in each annulus is integrated over a log-normal distribution, whose width is  $\ln(10)\sigma_T/\sqrt{2}$ . The local spectrum is assumed to be a colour-corrected blackbody with  $f = 1.7$  (e.g., Shimura & Takahara 1995).

In the following sections, this stationary log-normal model is used for spectral calculations and the rms variability is estimated from equation (1). Using the log-normal model is valid for  $n \gtrsim 30$ . Except in the brief discussion of X-ray polarization in §6, all relativistic and viewing geometry effects on the observed spectra are ignored. Sample ID spectra are shown in the top panel of Figure 1.

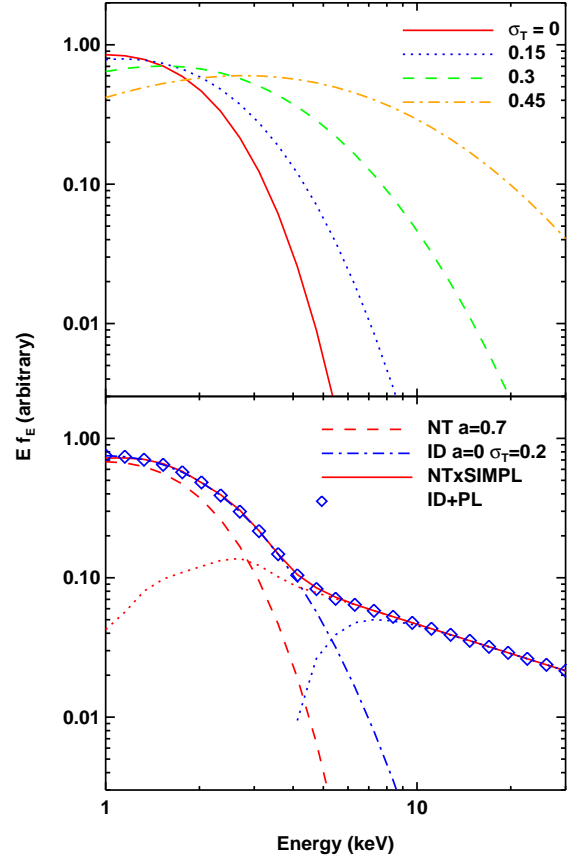


**Figure 1.** Top: X-ray spectra from the inhomogeneous disc (ID) model with  $a = 0.5$ . The spectra become harder and broader with increasing  $\sigma_T$ . Bottom: X-ray spectra from the NT (dashed) and NTxSIMPL (solid) models. A broader ID spectrum (dash-dotted line) with a power law tail (open diamonds) can appear nearly identical to the NTxSIMPL spectrum. The power law components are shown as dotted lines. The black hole mass is  $10M_\odot$ , and the SIMPL parameters are  $f_{SC} = 0.2$ ,  $\Gamma = 2.7$ .

## 3 THERMAL AND STEEP POWER LAW STATES

RM06 define three states of BHBs in terms of their spectral and variability characteristics. The hardness ratio, the ratio of integrated flux from 8.6 – 18.0 keV to that from 5.0 – 8.6 keV, and the rms variability are model-independent. The disc fraction is the ratio of the integrated disc to total flux between 2 – 20 keV. The disc flux is found by fitting spectra with the NT model, as well as a power law tail component with a corresponding photon index  $\Gamma$ .

Qualitatively, the ID models reproduce the observed trends in the TD to SPL states. For small  $\sigma_T \lesssim 0.1$ , the spectra are nearly identical to NT spectra. They are soft, disc-dominated, and exhibit little variability (TD state). As  $\sigma_T$  increases, the intrinsic disc spectrum becomes broader and harder (Figure 1). Fitting with a thin disc then requires an increasing degree of Comptonization, decreasing the disc fraction. The rms variability also increases with increasing  $\sigma_T$ . For large  $\sigma_T \gtrsim 0.3$ , the ID spectrum extends to energies  $\gtrsim 20$  keV and bears little resemblance to an NT spectrum, so that the disc fraction is small. The rms variability has also increased significantly. This is similar to the observed SPL state.

We demonstrate this quantitatively by treating the ID spectra as the data and least-squares fitting them with NT models along

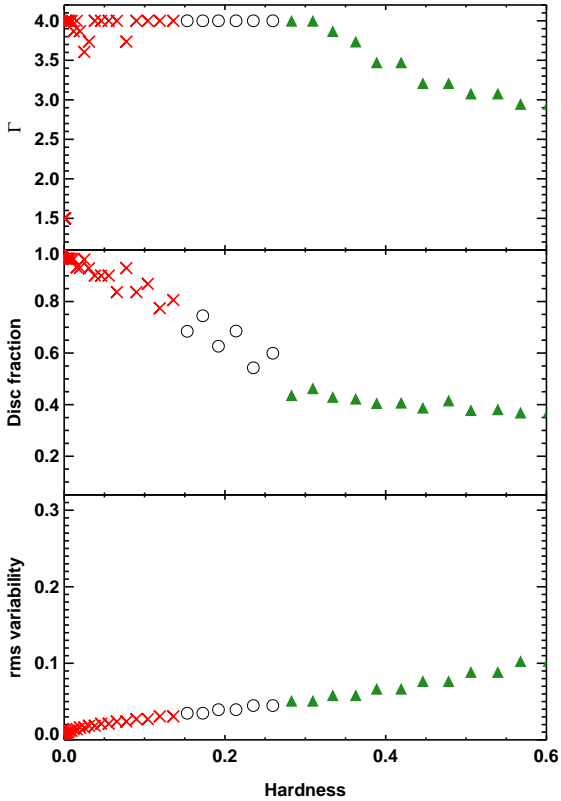


**Figure 2.** Inferred spectral and variability properties of ID models with  $a = 0.5$ . Quantities are defined and plotted as in panels e), f), and g) of Figs. 4-9 of RM06. Each point is the result of fitting an ID spectrum with parameters in the range  $\sigma_T = 0.02 - 0.5$  and  $\dot{m} = 0.8, 1.2$  with the NT $\otimes$ SIMPL model. The points are displayed according to their X-ray spectral state: thermal (red Xs), intermediate (open circles), and steep power law (green triangles).

with the SIMPL prescription for Comptonization (NT $\otimes$ SIMPL, Steiner et al. 2009b). With the simulated data and the parameters of the NT fits, we calculate the required RM06 parameters: hardness ratio and rms variability from the data (ID spectra), and the disc fraction and photon index  $\Gamma$  from the fits. The parameters of the ID (NT) spectra are  $a$ ,  $\dot{m}$ , and  $\sigma_T$  ( $a$ ,  $\dot{m}$ ,  $f_{\text{SC}}$ , and  $\Gamma$ ). For a given “source,” the black hole spin is fixed, while  $\dot{m}$  and  $\sigma_T$  vary. All of the NT parameters are allowed to vary. The normalized accretion rate is  $\dot{m} \equiv \dot{M}c^2/L_{\text{edd}}$ .

An example is shown in Figure 2. Each point represents a value of  $\dot{m}$  and  $\sigma_T$  from an ID spectrum with  $a = 0$ ,  $\dot{m} = 0.8, 1.2$ , and  $\sigma_T = 0.02 - 0.5$ , in 0.02 intervals. The number of ID zones,  $n$ , is set by requiring that the rms variability not exceed 15% in the SPL state for a range of ID spin values. The inferred value  $n = 1000$  is consistent with that required to explain optical/UV observations of AGNs (Figure 5 of DA11). The maximum value of  $\sigma_T$  that leads to an SPL spectrum is  $\simeq 0.5$ , identical to the maximum allowed by AGN observations. Using a smaller value of  $n$  would restrict the range of allowed  $\sigma_T$  (rms < 15%), preventing the model from describing the lowest disc fraction SPL states.

The results in Figure 2 are strikingly similar to the observed behavior of BHs (e.g., compare with Figure 4 of RM06). The relationship between disc fraction and hardness ratio is recovered with no free parameters. One point on the rms variability vs. hardness ra-

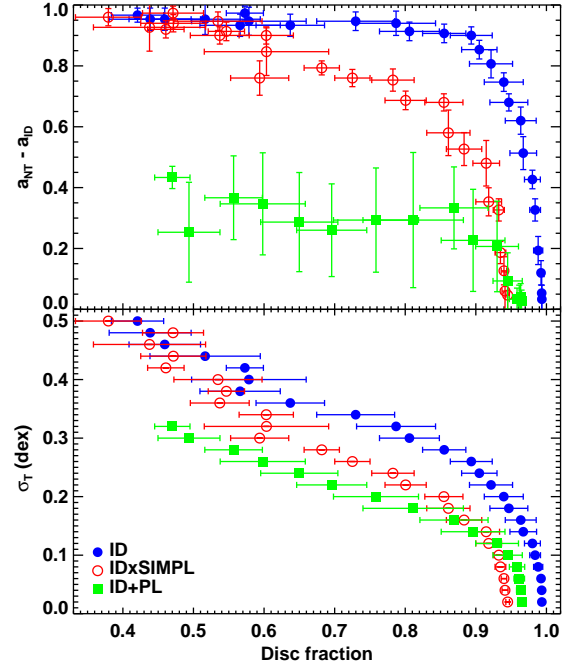


**Figure 3.** Top: Black hole spin inferred from fitting  $a = 0$  ID spectra with the NT $\otimes$ SIMPL model as a function of disc fraction. If the ID model correctly describes BHs, the NT interpretation of the data can significantly overestimate the true spin for disc fractions  $\lesssim 0.95$ . The magnitude of the effect is sensitive to the properties of the high energy spectral tail. Bottom:  $\sigma_T$  vs. disc fraction for the same fits. The disc fraction rapidly decreases for  $0.15 \lesssim \sigma_T \lesssim 0.35$ , where the ID spectra become significantly broader than their NT counterparts. The ID spectra either have no high energy tail (blue filled circles), a power law matched on arbitrarily above 5 keV (green filled squares), or a power law tail from SIMPL (red open circles) with  $f_{\text{SC}} = 0.03$ ,  $\Gamma = 2.5$ . The error bars are the ranges inferred from models with varying  $\dot{m}$  at fixed  $\sigma_T$ .

tio relation is fixed by the choice of  $n$ , but the predicted trend is also in agreement with observations. Different choices for ID spin,  $\sigma_T$ , and  $\dot{m}$  lead to variations of the same trends, and can explain much of the diversity observed in soft BHs. For example, the presence of distinct tracks in plots of disc fraction vs. hardness ratio (e.g., Figure 7 of RM06) can be explained as variations in  $\sigma_T$  at different values of  $\dot{m}$ . The inclusion of changes in  $n$  or possible correlations between  $n$ ,  $\sigma_T$ , and  $\dot{m}$  could cause additional scatter in Figure 2.

#### 4 POWER LAW TAIL MODELS

In the previous Section, the ID spectra were used as data without any power law spectral tail. This reduces the number of free parameters, but leads to steeper inferred photon indices than observed. The origin of this high energy tail emission is uncertain (e.g., Done, Gierliński & Kubota 2007). It can be modeled as a power law, often extending over all X-ray energies. However, at energies near the transition between disc and power law components, emission typically attributed to the power law could be due to a broader disc spectrum like that produced by the ID models.

The high energy tail can also be modeled with physical (Titarchuk 1994; Esin, McClintock & Narayan 1997) or empirical (Steiner et al. 2009b) Comptonization models. In both cases, the disc spectrum (or its Wien tail) is used as the seed photon spectrum,

implicitly assuming that the Comptonizing corona extends uniformly over the disc. This picture is strongly disfavored in AGNs by X-ray microlensing observations, where the corona is found to be much more compact than the optical/UV disc (Chartas et al. 2009; Dai et al. 2010). Steep radial emissivity profiles found from modeling X-ray reflection spectra in BHBs and AGNs (Miniutti & Fabian 2004; Schmoll et al. 2009) also favor a compact corona. There is no theoretical reason to expect large differences in coronal structure between AGNs and BHBs. All models for the high energy tail, then, introduce considerable uncertainty into BHB spectral fitting.

This uncertainty may allow the ID model of the SPL state to fit the data as well as the significantly Comptonized NT one. An example is shown in the bottom panel of Figure 1. The same spectrum (solid line) is produced by a significantly Comptonized NT $\otimes$ SIMPL, and a strongly inhomogeneous disc supplemented by a power law with a low energy cutoff at 5 keV (diamonds). This power law could mimic Comptonization from a compact corona. Recent radiative transfer calculations from relativistic MHD simulations have also found that emission from the plunging region, neglected in the NT model, can lead to a power law spectral tail (Zhu et al. 2012). Whatever the emission mechanism or geometry, the ID model for BHBs still requires that the normalization of the high energy tail increases with decreasing disc fraction (increasing  $\sigma_T$ ). ID spectra alone cannot explain the strong, non-thermal emission extending to 1 MeV in some SPL states.

## 5 IMPLICATIONS FOR BLACK HOLE SPIN MEASUREMENTS VIA CONTINUUM FITTING

One promising method for measuring black hole spin is to fit disc-dominated BHB spectra with the NT $\otimes$ SIMPL model. The hardness (or characteristic temperature) of the disc spectrum depends on its inner edge, which is assumed to coincide with the marginally stable orbit of the black hole. This allows a measurement of the spin, provided that the mass, inclination, and distance are accurately determined. This technique has been used to estimate the spins of several BHBs (e.g., McClintock et al. 2011).

In the ID model, the characteristic temperature increases with both increasing spin and  $\sigma_T$ . Therefore, if BHB accretion discs are inhomogeneous, the use of the NT model could introduce systematic errors in CF spin measurements. From the fitting procedure used in §3, the magnitude of these errors can be estimated as a function of the inferred disc fraction. The results are shown in the top panel of Figure 3 for an ID model with  $a = 0$ . The range of  $\sigma_T$  used is the same as in Figure 2, and is consistent with that favored by optical/UV AGN observations ( $0.35 < \sigma_T < 0.50$ , DA11).

The inferred spin using the NT model is always larger than the “true” ID spin, since the spectral peak moves to higher frequencies with increasing  $\sigma_T$ . Quantitatively, the spin differences depend on the high energy tail model used. This is because the spin and the SIMPL scattering efficiency  $f_{SC}$  both harden the spectrum. Without any high energy tail (blue filled circles),  $f_{SC}$  is small for  $\sigma_T < 0.15$  and instead the NT spin increases to fit the intrinsically harder ID spectra. A power law matched on smoothly to the ID spectrum above 5 keV (green filled squares) leads to a higher power law normalization with increasing  $\sigma_T$ . In that case,  $f_{SC}$  must increase to fit the tail, and much smaller changes in spin can explain the harder ID spectra. The disc fraction decreases sharply for  $\sigma_T \gtrsim 0.15$  as the ID spectra become broad, requiring significant Comptonization of the NT spectra in the fits (bottom panel of Figure 3). This leads to the sharp transition in inferred spin below disc

fraction  $\simeq 0.93 - 0.97$ , where the transition value depends on the high energy tail model.

## 6 DISCUSSION

X-ray spectral and timing observations of BHBs have established a set of states common to many objects. The physical origin of the SPL state and the cause of state transitions remain poorly understood. We have shown that the spectral and rms variability properties of soft, luminous BHBs (TD to SPL states) can be explained by varying one parameter: the amplitude of local temperature fluctuations in an inhomogeneous accretion disc. Comparable temperature fluctuations in quasar accretion discs can resolve a number of important observational puzzles in AGNs (DA11). The ID model then provides a unified picture of luminous black hole accretion discs across many orders of magnitude in black hole mass.

The most likely physical processes for driving large temperature fluctuations are radiation pressure dominated disc instabilities. Local MHD simulations are consistent with the thin disc prediction for the relationship between surface density and stress (or temperature) when time-averaged (Hirose, Blaes & Krolik 2009). The simplest interpretation is that the disc is viscously unstable. If so, it would likely produce temperature fluctuations qualitatively similar to those in the ID model. This can be tested with radially-extended radiation MHD simulations. Alternatively, large fluctuations could also occur in magnetically-dominated discs (e.g., Begelman & Pringle 2007), where the disc radiation energy content is de-coupled from its stability.

The ID model is insufficient to fit the X-ray spectra observed in both AGNs and BHBs. The broad ID spectrum produces some, but not all, of the emission typically attributed to the high energy tail, and some prescription for the remaining emission is still required. This could be from Comptonization in a compact corona or from hot gas inside the disc marginally stable orbit (Zhu et al. 2012). As with other models, the high energy tail normalization must increase with decreasing disc fraction in order to explain SPL spectra. Quantitative fitting of the ID spectral model to observations will be carried out in future work, with various prescriptions for the high energy tail. Spectral models could use the colour-corrected blackbody used here, or could incorporate the results of sophisticated accretion disc atmosphere calculations (BHSPEC, Davis et al. 2005; Davis & Hubeny 2006).

If BHBs are indeed inhomogeneous, spin measurements from current CF methods using the NT model are potentially subject to large systematic uncertainties (spin differences  $\Delta a \sim 0.3 - 0.9$  for ID spin  $a = 0$ , Figure 3). These can be much larger than current statistical uncertainties and systematic errors from ignoring emission from the plunging region ( $0.2 - 0.3$ , Kulkarni et al. 2011; Noble et al. 2011), except in the most disc-dominated states (disc fraction  $\gtrsim 0.95$  or  $\sigma_T \lesssim 0.15$ ). Therefore, if BHB discs are significantly inhomogeneous, spin measurements using CF methods should be restricted to the most disc-dominated states.

The ID model also generically predicts that the inferred spin using NT models should increase with decreasing disc fraction. Steiner et al. (2009a, 2010, 2011) have found that inferred spins in a few sources do not change significantly over a wide range of  $L/L_{\text{edd}}$  or  $f_{SC}$ . Since  $f_{SC}$  is a proxy for disc fraction, this latter conclusion is in apparent conflict with our Figure 3 (particularly Figure 1 of Steiner et al. 2009a). However, the magnitude of the inferred spin differences when fitting NT models to ID spectra depends sensitively on the high energy tail model assumed. Further,

the inferred spin from fitting ID models is nearly constant outside of a critical range in disc fraction. Observations of IDs entirely above (below) this range in disc fraction could find a constant, correct (incorrect) spin value, although there is no evidence for sharp changes in spin from CF at disc fractions  $\simeq 0.95$ . Fitting X-ray spectra with the ID model will allow estimates of  $a$  and  $\sigma_T$  in a variety of states, and test the model. Requiring the spin to be independent of spectral state may constrain  $\sigma_T$  and the degree of inhomogeneity in BHB accretion discs.

X-ray polarization measurements may provide another test for inhomogeneous accretion discs in BHBs. Assuming a semi-infinite scattering-dominated atmosphere (Chandrasekhar 1950), we have calculated polarized images and spectra via ray tracing using the codes GEOKERR (Dexter & Agol 2009) and GRTRANS (Dexter 2011). We account for all relativistic effects, including the rotation of the polarization vector (Connors, Stark & Piran 1980; Agol 1997). With these assumptions, the time-averaged ID polarization is unchanged from the NT model: 1–5% peak polarization, increasing strongly from face-on to edge-on viewing, and also increasing at lower black hole spin (Schnittman & Krolik 2009). X-ray polarization may then provide an additional constraint on the BH spin, independent of the location of the spectral peak. In addition, the polarization angle and degree vary by factors of a few on the fluctuation timescale. Both the degree of polarization and its time-variability increase with increasing  $\sigma_T$ . These estimates ignore returning radiation, as well as coronal (Schnittman & Krolik 2010) and plunging region (Agol & Krolik 2000) emission. These effects could cause additional differences between the polarization signatures of the ID and NT models.

The ID model used here assumes an optically thick disc. The NT effective optical depth is (e.g., Abramowicz & Fragile 2011):

$$\tau_{\text{NT}} \sim 1 \left( \frac{L}{L_{\text{edd}}} \right)^{-2} \left( \frac{R}{10M} \right)^{93/32}, \quad (3)$$

with  $G = c = 1$  and ignoring the effects of general relativity and of the inner disc edge on the optical depth. If the disc is inhomogeneous, portions will become optically thin. Assuming independent temperature and density fluctuations, we estimate the fraction of the disc with  $\tau_{\text{ID}} < 1$  by integrating the log-normal distribution,  $f(w)$ , for  $\tau_{\text{ID}}(w) = w^{2.3} \tau_{\text{NT}} < 1$ . For  $\sigma_T < 0.1$ ,  $\gtrsim 99\%$  of the disc is optically thick where the bulk of the luminosity is produced for  $L/L_{\text{edd}} \leq 1$ . At larger  $\sigma_T$ , the inner disc will become optically thin ( $\gtrsim 50\%$  by area at the peak emission radius for  $\sigma_T > 0.35$  and  $L/L_{\text{edd}} = 1$ ). If this emission is similar to that from the plunging region (Zhu et al. 2012), it could lead to the observed increasing high energy tail emission with decreasing disc fraction. Comptonization from hot electrons in optically thin regions may also effectively truncate the disc spectrum as inferred in the SPL state (Done & Kubota 2006).

## ACKNOWLEDGEMENTS

JD thanks E. Agol, O. Blaes, J. McClintock, J. Steiner, and J. Tom-sick for useful discussions. EQ is supported in part by the David and Lucile Packard Foundation.

## REFERENCES

Abramowicz M. A., Fragile P. C., 2011, arXiv:1104.5499  
 Agol E., 1997, PhD thesis, University of California, Santa Barbara

Agol E., Krolik J. H., 2000, ApJ, 528, 161  
 Balbus S. A., Hawley J. F., 1991, ApJ, 376, 214  
 Begelman M. C., Pringle J. E., 2007, MNRAS, 375, 1070  
 Belloni T., Mendez M., King A. R., van der Klis M., van Paradijs J., 1997, ApJ, 488, L109  
 Chandrasekhar S., 1950, Radiative transfer. Oxford, Clarendon Press  
 Chartas G., Kochanek C. S., Dai X., Poindexter S., Garmire G., 2009, ApJ, 693, 174  
 Connors P. A., Stark R. F., Piran T., 1980, ApJ, 235, 224  
 Dai X., Kochanek C. S., Chartas G., Kozłowski S., Morgan C. W., Garmire G., Agol E., 2010, ApJ, 709, 278  
 Davis S. W., Blaes O. M., Hubeny I., Turner N. J., 2005, ApJ, 621, 372  
 Davis S. W., Hubeny I., 2006, ApJS, 164, 530  
 Dexter J., 2011, PhD thesis, University of Washington  
 Dexter J., Agol E., 2009, ApJ, 696, 1616  
 —, 2011, ApJ, 727, L24  
 Done C., Gierliński M., Kubota A., 2007, A&A Rev., 15, 1  
 Done C., Kubota A., 2006, MNRAS, 371, 1216  
 Eigenbrod A., Courbin F., Meylan G., Agol E., Anguita T., Schmidt R. W., Wambsgans J., 2008, A&A, 490, 933  
 Esin A. A., McClintock J. E., Narayan R., 1997, ApJ, 489, 865  
 Grove J. E., Johnson W. N., Kroeger R. A., McNaron-Brown K., Skibo J. G., Philips B. F., 1998, ApJ, 500, 899  
 Hirose S., Blaes O., Krolik J. H., 2009, ApJ, 704, 781  
 Hirose S., Krolik J. H., Blaes O., 2009, ApJ, 691, 16  
 Jiménez-Vicente J., Mediavilla E., Muñoz J. A., Kochanek C. S., 2012, ApJ, 751, 106  
 Kelly B. C., Bechtold J., Siemiginowska A., 2009, ApJ, 698, 895  
 Kelly B. C., Sobolewska M., Siemiginowska A., 2011, ApJ, 730, 52  
 Krolik J. H., Horne K., Kallman T. R., Malkan M. A., Edelson R. A., Kriss G. A., 1991, ApJ, 371, 541  
 Kulkarni A. K. et al., 2011, MNRAS, 620  
 Lightman A. P., Eardley D. M., 1974, ApJ, 187, L1  
 MacLeod C. L. et al., 2010, ApJ, 721, 1014  
 McClintock J. E. et al., 2011, Classical and Quantum Gravity, 28, 114009  
 Miniutti G., Fabian A. C., 2004, MNRAS, 349, 1435  
 Neilsen J., Remillard R. A., Lee J. C., 2012, ApJ, 750, 71  
 Noble S. C., Krolik J. H., Schnittman J. D., Hawley J. F., 2011, ApJ, 743, 115  
 Novikov I. D., Thorne K. S., 1973, in Black Holes (Les Astres Occlus), New York: Gordon and Breach  
 Penna R. F., McKinney J. C., Narayan R., Tchekhovskoy A., Shafee R., McClintock J. E., 2010, MNRAS, 408, 752  
 Remillard R. A., McClintock J. E., 2006, ARA&A, 44, 49  
 Schmoll S. et al., 2009, ApJ, 703, 2171  
 Schnittman J. D., Krolik J. H., 2009, ApJ, 701, 1175  
 —, 2010, ApJ, 712, 908  
 Shakura N. I., Sunyaev R. A., 1973, A&A, 24, 337  
 —, 1976, MNRAS, 175, 613  
 Shimura T., Takahara F., 1995, ApJ, 445, 780  
 Sorathia K. A., Reynolds C. S., Stone J. M., Beckwith K., 2012, ApJ, 749, 189  
 Steiner J. F., McClintock J. E., Remillard R. A., Gou L., Yamada S., Narayan R., 2010, ApJ, 718, L117  
 Steiner J. F., McClintock J. E., Remillard R. A., Narayan R., Gou L., 2009a, ApJ, 701, L83  
 Steiner J. F., Narayan R., McClintock J. E., Ebisawa K., 2009b, PASP, 121, 1279  
 Steiner J. F. et al., 2011, MNRAS, 416, 941  
 Titarchuk L., 1994, ApJ, 434, 570  
 Zheng W., Kriss G. A., Telfer R. C., Grimes J. P., Davidsen A. F., 1997, ApJ, 475, 469  
 Zhu Y., Davis S. W., Narayan R., Kulkarni A. K., Penna R. F., McClintock J. E., 2012, arXiv:1202.1530